Clinical Radiology (2009) **64**, 12–21

REVIEW

# Magnetic resonance spectroscopy of the brain: review of metabolites and clinical applications

**D.P. Soares[a,*], M. Law[b]**

[a]*Section of Radiology, Department of Surgery, Radiology, Anaesthetics, and Intensive Care, University Hospital of the West Indies, Mona, Kingston, Jamaica, and* [b]*Department of Radiology and Neurosurgery, Mount Sinai Medical Centre, New York, New York*

Received 10 January 2008; received in revised form 1 July 2008; accepted 8 July 2008

Magnetic resonance imaging (MRI) provides anatomic images and morphometric characterization of disease, whereas magnetic resonance spectroscopy (MRS) provides metabolite/biochemical information about tissues non-invasively *in vivo*. MRS has been used clinically for more than two decades. The major applications of this advanced MRI tool are in the investigation of neurological and neurosurgical disorders. MRS has also been used in the evaluation of the prostate gland and muscle tissue, but these applications will not be addressed in this review. The aim of this review is to attempt to introduce the technique, review the metabolites and literature, as well as briefly describe our clinical experience.


## Introduction

Magnetic resonance imaging (MRI) was introduced in the mid-1970s and is based on the properties of nuclear magnetic resonance (NMR; used in chemistry to determine the structure of molecules). It was discovered independently by Bloch et al. at Stanford and Purcell et al. at Harvard in 1946.[1] To date, MRI provides the best soft-tissue contrast in diagnostic imaging.[2] Even with recent improvements in the contrast resolution, higher magnetic field strengths, and improved contrast media agents, tissue characterization remains limited. For example, the differentiation between a cerebral infarction and a low grade glioma can be difficult even with MRI, these entities having different clinical implications. The principles of NMR were further investigated to develop magnetic resonance spectroscopy (MRS), which then enabled such differentiation.[3]

The main difference between standard MRI and MRS is that the frequency of the MR signal is used to encode different types of information. MRI uses high spatial resolution to generate anatomical images, whereas MRS provides chemical information about the tissues. Spatial location determines the frequency with MRI, whereas the tissue's chemical environment determines the frequency in MRS.[4] Rather than images, MRS data are usually presented as line spectra, the area under each peak representing the relative concentration of nuclei detected for a given chemical species. The *x*-axis denotes the frequency shift localizing the metabolite in parts per million (Fig. 1).

Initially, MRS was technically difficult, but in 1995 the Food and Drug Administration (FDA) approved a fully automated, rapid, and inexpensive MRS sequence for neuro-MRS, the so-called PROBE sequence: PROton Brain Examination; the acronym chosen for localized, single voxel hydrogen ion (proton) spectroscopy. This PROBE sequence runs without intervention by the physicist and minimal intervention by the MR technologist.

* Guarantor and correspondent: D. P. Soares, Section of Radiology, Department of Surgery, Radiology, Anaesthetics and Intensive Care, University Hospital of the West Indies, Mona, Kingston 7, Jamaica. Tel./fax: +876 9775277/9271933.
*E-mail address:* dpsoares@cwjamaica.com (D.P. Soares).

0009-9260/$ - see front matter © 2008 The Royal College of Radiologists. Published by Elsevier Ltd. All rights reserved.
doi:10.1016/j.crad.2008.07.002

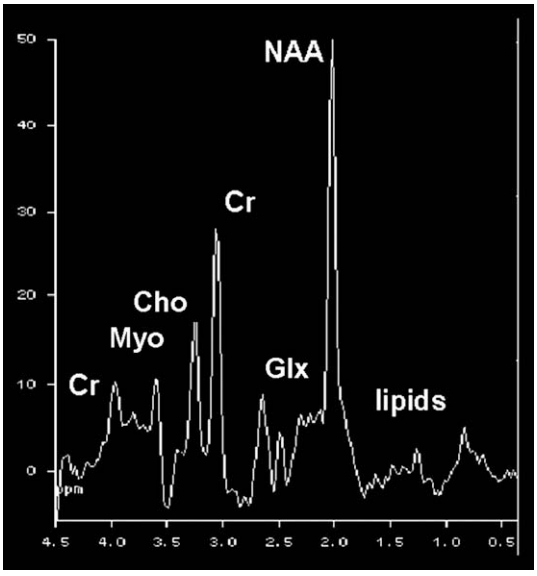


**Figure 1** Normal spectrum at short TE. Spectrum demonstrates major metabolites, such as NAA peak at 2.02, Cho peak at 3.22, and Cr, which has peaks at 3 and 3.9 ppm. At short TE, metabolites with shorter T2 decays will be demonstrated, such as Myo at 3.6 ppm, Glx at 2.05—2.5 ppm, and sometimes some lipid peaks at 0.9 and 1.3 ppm.

It provides a proton spectrum for the chosen volume of interest in 6 min or less.[3]

Protons are more commonly used for spectroscopy because of their high natural abundance in organic structures and their high magnetic sensitivity when compared with other nuclei, such as phosphorus, sodium, carbon, fluorine, and lithium,[5] which require specialized coils and amplifiers for observation. By comparison proton MRS uses the same hardware as standard MRI.[6] Spectroscopy may be performed using a single voxel technique (single voxel spectroscopy), or multiple voxels, sometimes known as magnetic resonance spectroscopic imaging (MRSI) or chemical shift imaging (CSI).[7] The term voxel refers to the volume being sampled. Both two and three-dimensional localization techniques are clinically available.

Proton spectroscopy may be obtained with most modern MRI systems. These systems can perform MRS without additional hardware, provided they have the capability of shimming (i.e., optimizing field homogeneity). However, MRS is not possible below a field strength of 1 T. The development of spatially localized MRS[8—10] has provided a bridge between metabolism and the anatomic and physiological studies available from MRI. Localization can be achieved in MRS by using narrowband radiofrequency pulses in conjunction with pulsed spatial gradients among other methods, which are beyond the scope of this text.[8—10] However, these developments facilitate a single MR examination that has anatomic, physiological, and metabolic information. Distinct lesions can be further categorized, and response to treatment evaluated. Where no discrete lesions are seen, the underlying metabolic status of grey and white matter tissue being studied can be interrogated.[6]

## The spectrum

MRS provides *in vivo* biochemical information. The peaks on the spectra obtained correspond with various metabolites, normal and abnormal, which may be identified precisely. Although peaks from non-identical molecules may overlap, in clinical practice, this is not usually an issue where brain metabolites are concerned, [3,11] particularly when scanning at 1.5 T (at higher field strengths this is not necessarily the case). Proton spectra are displayed on *x* and *y* axes. The horizontal *x* axis, plots the frequency chemical shift in parts per million of the various metabolites in a given tissue sample. The vertical *y* axis plots the relative signal amplitude or concentrations for the various metabolites, i.e., the height of the peak reflects the amount of the metabolite. Spectra are read from right to left, the numbers (ppm) on the *x* axis increasing in the same direction (i.e., right to left).

The metabolites that can be identified with proton MRS are, in part, dependent on the echo time (TE). At 1.5 T, metabolites visualized utilizing intermediate to long TE (144—288ms) include N-acetylaspartate (NAA), choline (Cho), creatine (Cr), possibly alanine (Ala), and lactate.[12,13] Short echo-time acquisitions ($TE < 40$ ms) include the above metabolites as well as myoinositol (Myo), glutamate and glutamine (Glx), glucose (Gc), and some macromolecular proteins and lipids[13] (Fig. 1). Concentrations of normal metabolites in the brain vary slightly in different age groups. Generally, by the time a child is 2-years-old it will have a spectral pattern similar to an adult. Prior to that age, the most striking variation is a reversal in the NAA:Cr ratio and the Cho:Cr ratio.[14] As the brain matures, the concentration of NAA increases and the concentration of Cho decreases. In the elderly, there is a normal decline in the level of NAA.

## NAA

NAA is present in relatively large quantities in the normal brain parenchyma and is, therefore, the highest peak in the normal spectrum, resonating at

2.02 ppm. With good resolution, second and third peaks of NAA can be observed (at 2.6 and 2.5 ppm). NAA is produced in the mitochondria of the neurons and transported into the neuronal cytoplasm. The exact role of NAA is presently not known (despite more than 40 years of investigation), but it continues to be used as a marker of neuronal density and viability. NAA can also be found in immature oligodendrocytes and astrocyte progenitor cells.[15] There is normally an increase in NAA in grey matter from ventral to dorsal, and from the cerebral hemispheres to the spinal cord.[16]

NAA is also found in axons as it is transported along axons from the site of synthesis in the neuronal mitochondria, hence it is found in both grey and white matter (in approximately equal quantities).[3] The utility of NAA as an axonal marker is supported by the loss of NAA in many white matter diseases, including leukodystrophies, multiple sclerosis (MS), and hypoxic encephalopathy.[6] Malignant tumours cause destruction of neurons and thus a loss of NAA and purely extra-axial lesions, such as typical meningiomas, demonstrate no NAA.[17] The only known disease to exhibit an increase in NAA is Canavan's leukodystrophy.[12]

There are suggestions in the literature that NAA is a cerebral osmolyte.[18–23] This may imply that NAA changes might be reversible, an observation that has been made in conditions such as MS, acquired immunodeficiency syndrome (AIDS), and temporal lobe epilepsy.[24]

## Cho

Cho is a metabolic marker of membrane density and integrity, i.e., phospholipids synthesis and degradation, with its peak located at 3.22 ppm. The water soluble precursors of membranes, choline and phosphocholine, that remain free (i.e., those that are not incorporated into the large macromolecules on the surface of the membrane) will be seen at spectroscopy.[3,11] There are different levels of choline in grey and white matter. Malignant tumours show an increase in the choline peak because of increased cellularity. Increases in Cho relative to NAA and Cr are also noted with cerebral infarctions, inflammation and MS, and hence in itself, is not a specific finding.[3,25] Therefore, difficulty may be encountered in interpreting results in some lesions, such as tumefactive MS.[26–29] However, compared with tumoural disease, there is generally a decrease in Cho compared with the contralateral normal Cho in non-tumoural pathology.

## Cr

In simplistic terms, Cr is a marker of ''energy metabolism''. The central peak on the spectrum at 3.02 ppm represents the sum of creatine and phosphocreatine. In the clinical setting, Cr is assumed to be stable and is used for calculating metabolite ratios (Cho:Cr and NAA:Cr ratios).[3] However, regional and individual variability in Cr concentration is known, and, particularly in the research setting, absolute metabolite quantification may increase the sensitivity and specificity of MRS.[30] Cr is known to be reduced in tumours due to the increased metabolic activity of the tumours, particularly high-grade gliomas.[31] It may be useful to note that Cr itself does not originate in the brain, and hence systemic disease (such as renal disease) may impact on Cr levels in the brain.[3] There has also been at least one report of a new inborn error of Cr biosynthesis that manifested as an absence of Cr from the proton spectrum. This deficiency was corrected by dietary administration of Cr.[32]

## Glx

Glutamate (Glu), Glutamine (Gln) and gamma-aminobutyric acid (GABA) are generally inseparable at 1.5 T and result in a complex of peaks (Glx) between 2.05 and 2.5 ppm. Glu is an excitatory neurotransmitter, being the most abundant neurotransmitter in the brain. Glu and Gln play a role in detoxification and regulation of neurotransmitters. Glu, which is viewed as an important neurotoxin when its concentration exceeds that needed for neuro-transmission, is also a participant in the redox cycle.[3] Other metabolites contribute to the signal at the chemical shift of Glu:Gln, making precise determination of their concentrations difficult at 1.5 T. The use of higher field strengths may ultimately be able to improve quantitation of these compounds.[33–37]

## Lactate

Under normal circumstances, lactate is present only in minute amounts in the brain and is not resolved using the normal spectroscopic techniques. However, under conditions where the aerobic oxidation mechanism fails and anaerobic glycolysis takes over, such as brain ischaemia, hypoxia, seizures, metabolic disorders, and with macrophage accumulation (areas of acute inflammation), lactate levels increase significantly.[38] Lactate also accumulates in tissues that have poor washout, like cysts and necrotic and cystic tumours, as well as normal pressure hydrocephalus.[39]

When present, it is recognized as a doublet (twin peak) at 1.33 ppm. Lactate is characterized by variable projection of the peak at different TEs. On acquisitions using intermediate TEs (135/144ms), the doublet peak is inverted below the baseline, but at very short or very long TE (30 or 288 ms), the doublet peak projects above the baseline.[12,13]

### Myo

Myo is a simple sugar, with a peak found at 3.56 ppm. It is absent from neurons. In the brain, it is synthesized primarily in glial cells and cannot cross the blood—brain barrier.[40,41] It is considered a glial marker.[12] It is found almost exclusively in astrocytes where it is recognized as an important osmolyte[42] or astrocytic marker.[3] An increase in Myo content is believed to represent glial proliferation or an increase in glial cell size, both of which may occur in inflammation.[6] It is elevated in the setting of gliosis, astrocytosis, and in disorders such as Alzheimer's dementia. Myo has also been labelled as a breakdown product of myelin.[43]

### Ala

Ala is a metabolite with uncertain function with a doublet peak at 1.48 ppm, but its presence may be overshadowed by lactate, which resonates at 1.33 ppm. It has a role in the citric acid cycle and may be found in some meningiomas.[12,13]

### Lipids

Membrane lipids have very short relaxation times and are not usually visualized on intermediate or long TE, but are visualized on short TE.[44] They produce peaks between 0.8 and 1.5 ppm and are usually large broad peaks. The presence of lipids may indicate voxel contamination by diploic space fat, scalp and subcutaneous tissues (when the voxel is placed near these structures).[12]

## The clinical experience

To perform MRS one does not need to purchase a unit dedicated to such a purpose. As long as the field strength is adequate and the appropriate packages are purchased, most clinically available MRI systems with field strengths of 1 T or greater, may be used. There is no additional patient preparation. The patient is required to remain still for the duration of sampling of each region of interest, which at our institution is roughly 4 min for single voxel spectroscopy. Patients for seizure evaluation have routine brain images done, as well as sampling of both hippocampal areas at the level of the red nucleus in the coronal plane. The entire procedure takes roughly 30 min. For other conditions, routine images would also be done, but the region sampled may vary depending on the question to be answered.

### Clinical applications

One of the earliest applications of MRS was in the differentiation of low-grade gliomas from infarction. This is a common diagnostic dilemma in the young stroke patient with no predisposing factors for cerebral infarction. Whereas tumours would have a predominant Cho peak and almost absent NAA, infarction would have a predominant lactate peak and an overall reduction in metabolites, both Cho and NAA (Fig. 2). High-grade gliomas may have prominent lactate peaks, however, the imaging findings would tend not to simulate infarction. Major indications for MRS remain in the evaluation of patients with neurological and neurosurgical disorders.

### Tumour evaluation

Hydrogen (proton) spectroscopy proved successful in differentiating malignant brain tumours from normal brain tissue in adults as well as children.[45,46] The basic metabolite changes common to brain tumours include elevation in Cho, lactate, and lipids; and decrease in NAA and Cr. The

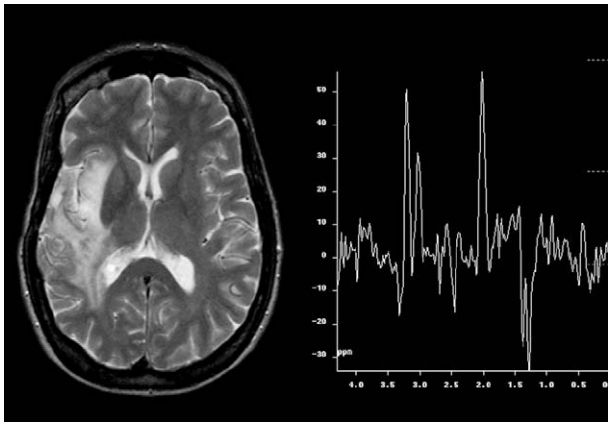

**Figure 2** A patient with a right temporoparietal infarct. (a) Axial T2-weighted image demonstrating increased signal involving the grey and white matter in the right middle cerebral artery territory in keeping with acute ischaemia. (b) Intermediate TE (135 ms) spectrum demonstrating decreased NAA and elevation in Cho with inversion of a large lactate doublet, in keeping with anaerobic metabolism seen in acute infarction.

increase in Cho is attributed to cell membrane turnover and proliferation.[3,12,13,45,47–51] Cho metabolism is complex and beyond the scope of this text, however, the release of phosphorylcholine and glycerophosphorylcholine from cell membrane destruction and the production of these metabolites during cell membrane synthesis are thought to be the biochemical basis for Cho elevation. In proton spectroscopy, an elevation in Cho may be due to cell membrane synthesis, destruction or both. In lymphoma, there is typically elevation in Cho as well as lipid and lactate (Fig. 3).

Measurable levels of Cho vary considerably, depending on cellular density, tumour grade and presence or absence of necrosis.[47,52,53] Cho resonance is most prominent in regions with high neoplastic cellular density, and is progressively lower in moderate and low-grade tumours.[47–49,52–55] Paradoxically, some highly malignant tumours, for example, a glioblastoma multiforme, may show low Cho because of extensive necrosis.[12,13] The range of Cho levels may show intra-tumoural variation due to the presence of different histological grades within the lesion, haemorrhage, calcifications, or areas of radiation necrosis in the treated patient.

The grading of gliomas has significant clinical importance, as high-grade gliomas are usually treated with adjuvant radio- or chemotherapy after resection, whereas low-grade gliomas are not. Histopathological assessment, the current reference standard for tumour grading, has limitations, such as inherent sampling error associated with the limited number of biopsy samples. Even with cytoreductive surgery, histology can only be performed on excised tumour, and residual tumour cannot be examined. Importantly, it is well known that residual low-grade tumour has the propensity for malignant transformation. The histopathological classification of gliomas itself is a controversial subject, under constant discussion and revision.[56] High-grade gliomas generally have higher Cho levels than low-grade gliomas.[57] Recently, the percent change in the ratio of Cho:NAA has been shown to be useful in predicting tumour progression in children with brain tumours.[58]

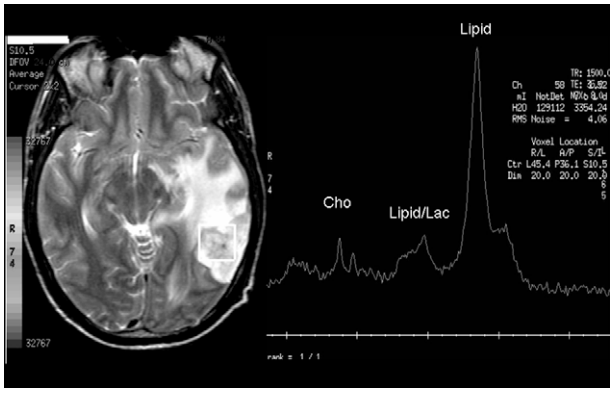


**Figure 3** An adult male patient with a history of non-Hodgkin's lymphoma treated with radiation therapy. (a) Axial T2-weighted image demonstrating abnormal signal in the left temporo-parietal region with involvement of the peri-ventricular white matter. The location of the region of interest for the single-voxel MR spectroscopy is also shown. (b) Short echo (TE 35 ms) MRS of the lesion showing predominant lipid and lactate peaks suggesting coagulative necrosis. There is also some elevation in Cho.

A review of the literature, taking into account differences in spectroscopic technique, such as the choice of TE and method for determination of metabolite ratios, demonstrates maximal values for NAA:Cr to be of utility in differentiating between low and high-grade gliomas.[48,59–62] There are differences in Cho levels between low and high-grade gliomas, with low-grade gliomas generally demonstrating lower Cho levels than high-grade gliomas.[57] This difference is appreciated even using different methods for quantifying Cho.[63,64]

McKnight et al.[65] demonstrated 90% sensitivity and 86% specificity by using a Cho:NAA statistical index (CNI) of 2.5 distinguishing tumoural tissue from non-tumoural tissue. The median CNI values for grade II/IV, grade III/IV and grade IV/IV gliomas are 6.9, 7.1, and 9.37, respectively, with a large variation in the maximum CNI in the grade IV/IV group.[66] In comparing spectroscopy with conventional MRI, Law et al.[57] demonstrated a threshold value of 1.56 for Cho:Cr to provide sensitivity, specificity, positive predictive and negative predictive values of 75.8, 47.5, 81.2, and 39.6%, respectively, for the determination of a high-grade glioma value versus a low-grade glioma ($n = 160$). In the same study, a threshold value of 1.6 for Cho:NAA provided 74.2, 62.5, 85.6, and 44.6% for the sensitivity, specificity, positive and negative predictive values, and 72.5, 65, 86.1, and 44.1%, respectively, for conventional MRI in predicting a high-grade glioma.

The clinical utility of tumoural proton MRS in glioma grading is still being investigated. At this point, it is important to understand that MRS is very sensitive to abnormal metabolic changes, but the specificity is relatively low.[67] Clinically it is not uncommon to find some low-grade gliomas with very high Cho:Cr and Cho:NAA ratios, and conversely, high-grade gliomas with lower Cho:Cr and Cho:NAA ratios, due primarily to extensive necrosis, which increases the false-positive rate

and false-negative rates, respectively. There is some overlap in CNI between tumours of different grades.[66] It may also be related to the variability in using metabolite ratios rather than absolute quantification to compare glioma grades.[30,68] Lipid and lactate elevation correlate with necrosis in high-grade gliomas and have also been shown to be useful in differentiating low and high-grade gliomas.[45,48,69,70] Using short echo MRS (TE 20—30 ms), Myo can also be used to differentiate low and high-grade gliomas.[7,59,71] Low-grade gliomas express higher levels of Myo compared with high-grade gliomas. This may be due to the lack of activation of phosphatidylinositol metabolism resulting in accumulation of Myo. Combining MRS and perfusion MRI improves the sensitivity to 93.3% compared with 72.5% for conventional MRI alone.[57] However, it is now widely appreciated that because of the heterogeneity of tumours, there is significant overlap between whatever spectroscopy indices are used to grade gliomas.[71]

## Seizure disorders

Epilepsy is a common disorder with an estimated prevalence of 0.8%.[72] The most common seizure types are complex partial seizures.[73] The term ''complex'' indicates loss or alteration of consciousness during a seizure. ''Partial'' refers to a focal seizure originating in part of the brain. In approximately 80% of patients, the seizure originates in the temporal lobe. Patients with intractable seizures which are difficult to control medically, are potential candidates for surgery if the focus of abnormal electrical activity can be reliably identified.

MRI is commonly performed in patients with seizure disorders. Hippocampal sclerosis may be implicated in such patients 60—85%, and may be diagnosed using MRI.[74—77] There are different parameters that are important in making such a diagnosis, notably the size and signal intensity of the hippocampi. Hippocampal sclerosis may be characterized by a decrease in volume of the hippocampus involved, as well as an increase in signal intensity on T2WI. However, these findings may be absent or equivocal in the seizure patient. Spectroscopy can be used to add diagnostic sensitivity, demonstrating decreased NAA and elevation of Glx and Myo in hippocampal sclerosis. These findings may be seen in hippocampi that demonstrate symmetry in size and no increase in signal intensity (Fig. 5). Correlation with electroencephalography is advised in all cases.

## Evaluation of the patient with suspected dementia

Imaging has an important role in evaluating patients with suspected dementia. Subdural haematomas, multiple cerebral infarctions, as well as normal pressure hydrocephalus, can all present with symptoms suggestive of dementia. It is clinically important to positively identify or exclude these entities, if possible, as the management of these conditions varies significantly as do the prognoses. Alzheimer's dementia, often treated as a diagnosis of exclusion, with the definitive diagnosis only possible at autopsy, can sometimes be positively identified with the aid of MRI and MRS (Fig. 4).[78] MRI can sometimes demonstrate cerebral atrophy more marked in the temporal lobes in these patients. At spectroscopy, there is a decrease in NAA levels, as well as an increase in Myo, in the occipital, temporal, parietal, and frontal regions of patients with Alzheimer's dementia.[79] MRS has recently been shown to be capable of diagnosing mild cognitive impairment (MCI), which has been recognized as a condition that can precede Alzheimer's dementia. MRS is also thought capable of predicting which patients with MCI will develop Alzheimer's dementia.[80—83] Detecting these early changes is becoming more important as pharmacological intervention for Alzheimer's becomes increasingly effective. Although at times it may be difficult to confirm the diagnosis, serial scans may be useful to monitor changes in metabolite levels.

## Evaluation of the comatose patient

Spectroscopy has also been used in determining the underlying cause of comas. For example,

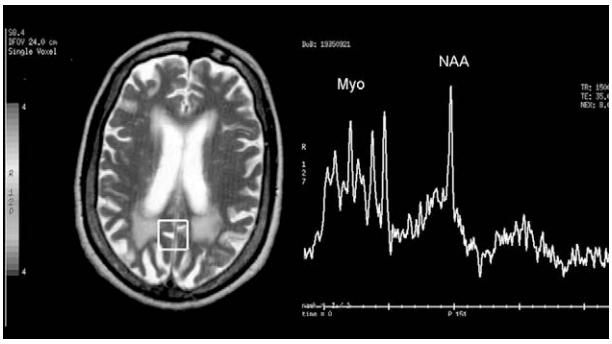


**Figure 4** An elderly patient with increasing memory loss. (a) Axial T2-weighted image showing cerebral atrophy, as well as some periventricular T2 signal change, in keeping with some microvascular disease. (b) Short echo (TE 35 ms) MRS of the parietal grey matter demonstrating decreased NAA and increased Myo in keeping with Alzheimer's dementia.

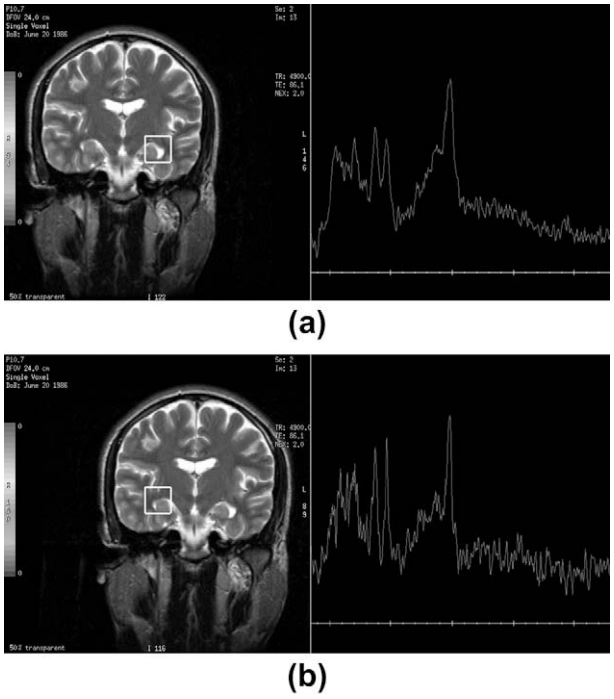


**Figure 5** A 20-year-old male patient with a diagnosis of epilepsy. Coronal T2-weighted images showing essentially normal hippocampi and their respective spectra. Short echo (TE 35ms) MRS demonstrating bilaterally decreased NAA and increased Myo, more severe on the right, suggestive of bilateral hippocampal sclerosis.

hepatic encephalopathy has its own unique spectroscopic signature. In hepatic encephalopathy, Myo would be absent, Cho reduced, and Glu increased.[3] In the comatose patient post-head injury, one would expect a mild to moderate decrease in NAA. The absence of lactate would exclude severe hypoxic injury. In the patient in a prolonged coma, severely decreased NAA and persistent lactate would suggest a poor prognosis.[3]

## Our experience

In December 2001, we acquired a 1.5 T Signa Smartspeed, GE medical Systems. Among its capabilities is that of MRS. We routinely obtain short TE single voxel spectra. For seizures, both hippocampi are sampled using coronal localizers at the level of the red nuclei. For suspected dementia, parietal white and grey matter are sampled (Fig. 4). For suspected tumours, we also undertake single voxel sampling, as well as multi-voxel spectroscopy, one or more voxels in a representative area of the suspected lesion, and corresponding ROIs on the contralateral side. Multiple samples may be performed depending on the size and apparent characteristics of the lesion. Intermediate TE spectra (144) are obtained when there is a need to confirm the presence of lactate. The advantage of multivoxel MRS is the ability to provide multiple samples, compare abnormal spectra with normal spectra in normal brain and to acquire multiple spectra in the same acquisition time.

To date we have investigated 137 cases using MRS; 92 cases have been in the evaluation of patients with seizure disorders, 20 for suspected dementia, and 25 for characterization of intracranial lesions. We have successfully differentiated tumours from infarction and radiation necrosis from recurrent tumours (Fig. 3). There has also been good correlation with clinical and EEG findings in some patients with seizure disorders. An audit of our cases is in progress to quantify overall sensitivity, as well as specificity, as our caseload increases.

## The future

A number of recent advances have reduced acquisition times, as well as improving signal:noise ratios. Several investigators have shown that the signal:noise ratio gains at 3 T and 4 T are relatively modest compared with theoretical predictions.[84] Scanning at higher field strengths has improved resolution, however, it is not without problems, and increases in resolution *in vivo* were degraded by increased line widths.[85]

Advanced MRI techniques, such as MR spectroscopy, diffusion and perfusion MRI can give important *in vivo* physiological and metabolic information, complementing morphological findings from conventional MRI in the clinical setting. Combining perfusion MRI and MRS will help in solving difficult cases and increase confidence in diagnosis. However, there is still need for caution in the final interpretation. These advanced MRI techniques are useful in both clinical and research settings; however, they should be considered supplementary tools to the patients' clinical history, examination, and conventional MRI when making a diagnosis. Ultimately, these tools can be used in a multiparametric, algorithmic fashion to characterize tissue biology.[86,87]

## References

1. Dendy PP, Heaton B. *Physics for diagnostic radiology*. 2nd ed. Bristol, Philadelphia, PA: Institute of Physics Publishing; 1999.
2. Zimmerman RA, Bilaniuk LT, Johnson MH, et al. MRI of central nervous system: early clinical results. *AJNR Am J Neuroradiol* 1986;**7**:587—94.

3. Danielsen ER, Ross B. *Magnetic resonance spectroscopy diagnosis of neurological diseases*. 1st ed. New York: Marcel Dekker, Inc; 1999.
4. Elster AD, Burdette JH. *Questions and answers in magnetic resonance imaging*. 2nd ed. St Louis: Mosby; 2001.
5. Lenkinski RE, Schnall MD. MR spectroscopy and the biochemical basis of neurological disease. In: Atlas SW, editor. *Magnetic resonance imaging of the brain and spine*. New York: Raven Press; 1991. p. 1099—121.
6. Rosen Y, Lenkinski RE. Recent advances in magnetic resonance neurospectroscopy. *Neurotherapeutics* 2007;**4**:330—45.
7. Law M, Cha S, Knopp EA, et al. Glioma grading with multi-slice, multi-voxel, multi-TE spectroscopic MRI and multi-slice perfusion MRI. Annual Meeting of the ISMRM, Hawaii, 2002.
8. Bolinger L, Lenkinski R. Localization in clinical NMR spectroscopy. In: Berliner LJ, Rueben J, editors. *Biological magnetic resonance*. New York: Plenum Press; 1992. p. 1—53.
9. Keevil SF. Spatial localization in nuclear magnetic resonance spectroscopy. *Phys Med Biol* 2006;**51**:R579—636.
10. Narayana PA, DeLayre JL. Localization methods in NMR. In: Partain CL, Price RR, Patton JA, Kulkarni MV, et al, editors. *Magnetic resonance imaging*. 2nd ed. Philadelphia: W.B. Saunders; 1988. p. 1609—30.
11. Ross B, Michaelis T. Clinical application of magnetic resonance spectroscopy. *Magn Reson Q* 1994;**10**:191—247.
12. Castillo M, Kwock L, Scatliff J, et al. Proton MR spectroscopy in neoplastic and non-neoplastic brain disorders. *Magn Reson Imaging Clin N Am* 1998;**6**:1—20.
13. Kwock L. Localized MR spectroscopy: basic principles. *Neuroimaging Clin N Am* 1998;**8**:713—31.
14. Ruggieri. Practical MR spectroscopy in paediatric neuroradiology. American Society of Neuroradiology, Advanced imaging symposium, Atlanta, 2000.
15. Urenjak J, Williams SR, Gadian DG, et al. Specific expression of N-acetylaspartate in neurons, oligodendrocyte-type-2 astrocyte progenitors, and immature oligodendrocytes *in vitro*. *J Neurochem* 1992;**59**:55—61.
16. Pouwels PJ, Frahm J. Regional metabolite concentrations in human brain as determined by quantitative localized proton MRS. *Magn Reson Med* 1998;**39**:53—60.
17. Bruhn H, Frahm J, Gyngell ML, et al. Noninvasive differentiation of tumors with use of localized H-1 MR spectroscopy *in vivo*: initial experience in patients with cerebral tumors. *Radiology* 1989;**172**:541—8.
18. Ross Bd, Colletti P, Lin A. Magnetic resonance spectroscopy of the brain: neurospectroscopy. In: Edelman RR, Hesselink JR, Zlatkin MB, Crues JV, editors. *Clinical magnetic resonance imaging*. Philadelphia: Saunders; 2006. p. 1840—901.
19. Baslow MH. Brain N-acetylaspartate as a molecular water pump and its role in the etiology of Canavan disease: a mechanistic explanation. *J Mol Neurosci* 2003;**21**: 185—90.
20. Baslow MH. N-acetylaspartate in the vertebrate brain: metabolism and function. *Neurochem Res* 2003;**28**:941—53.
21. Baslow MH. Evidence supporting a role for N-acetyl-L-aspartate as a molecular water pump in myelinated neurons in the central nervous system. An analytical review. *Neurochem Int* 2002;**40**:295—300.
22. Baslow MH, Hrabe J, Guilfoyle DN. Dynamic relationship between neurostimulation and N-acetylaspartate metabolism in the human visual cortex: evidence that NAA functions as a molecular water pump during visual stimulation. *J Mol Neurosci* 2007;**32**:235—45.
23. Bluml S, McComb JG, Ross BD. Differentiation between cortical atrophy and hydrocephalus using 1H MRS. *Magn Reson Med* 1997 Mar;**37**:395—403.
24. Barker Pb, Lin DDM. *In vivo* proton MR spectroscopy of the human brain. *Prog NMR Spectrosc* 2006;**49**:99—128.
25. Law M. *Magnetic resonance spectroscopy*. New York City: MRI: Clinical-State-of-the-Art; 2002.
26. Law M, Meltzer DE, Cha S. Spectroscopic magnetic resonance imaging of a tumefactive demyelinating lesion. *Neuroradiology* 2002;**44**:986—9.
27. Saindane AM, Cha S, Law M, et al. Proton MR spectroscopy of tumefactive demyelinating lesions. *AJNR Am J Neuroradiol* 2002;**23**:1378—86.
28. Ernst T, Chang L, Walot I, et al. Physiologic MRI of a tumefactive multiple sclerosis lesion. *Neurology* 1998;**51**: 1486—8.
29. Butteriss DJ, Ismail A, Ellison DW, et al. Use of serial proton magnetic resonance spectroscopy to differentiate low grade glioma from tumefactive plaque in a patient with multiple sclerosis. *Br J Radiol* 2003;**76**:662—5.
30. Li BS, Wang H, Gonen O. Metabolite ratios to assumed stable creatine level may confound the quantification of proton brain MR spectroscopy. *Magn Reson Imaging* 2003; **21**:923—8.
31. Lowry OH, Berger SJ, Chi MM, et al. Diversity of metabolic patterns in human brain tumors—I. High energy phosphate compounds and basic composition. *J Neurochem* 1977;**29**: 959—77.
32. Hanefeld F, Holzbach U, Kruse B, et al. Diffuse white matter disease in three children: an encephalopathy with unique features on magnetic resonance imaging and proton magnetic resonance spectroscopy. *Neuropediatrics* 1993;**24**: 244—8.
33. Mason GF, Pan JW, Ponder SL, et al. Detection of brain glutamate and glutamine in spectroscopic images at 4.1 T. *Magn Reson Med* 1994;**32**:142—5.
34. Pan JW, Mason GF, Pohost GM, et al. Spectroscopic imaging of human brain glutamate by water-suppressed J-refocused coherence transfer at 4.1 T. *Magn Reson Med* 1996;**36**: 7—12.
35. Ugurbil K, Adriany G, Andersen P, et al. Ultrahigh field magnetic resonance imaging and spectroscopy. *Magn Reson Imaging* 2003;**21**:1263—81.
36. Tkac I, Rao R, Georgieff MK, et al. Developmental and regional changes in the neurochemical profile of the rat brain determined by *in vivo* 1H NMR spectroscopy. *Magn Reson Med* 2003;**50**:24—32.
37. Srinivasan R, Cunningham C, Chen A, et al. TE-averaged two-dimensional proton spectroscopic imaging of glutamate at 3 T. *Neuroimage* 2006;**30**:1171—8.
38. Lopez-Villegas D, Lenkinski RE, Wehrli SL, et al. Lactate production by human monocytes/macrophages determined by proton MR spectroscopy. *Magn Reson Med* 1995;**34**: 32—8.
39. Kizu O, Yamada K, Nishimura T. Proton chemical shift imaging in normal pressure hydrocephalus. *AJNR Am J Neuroradiol* 2001;**22**:1659—64.
40. Font C, Garia-Campos M, Hansen AJ, et al. Simultaneous diffusion of inositol and mannitol in the rat brain. *Rev Esp Fisiol* 1982;**38**:317—9 [In Spanish].
41. Brand A, Richter-Landsberg C, Leibfritz D. Multinuclear NMR studies on the energy metabolism of glial and neuronal cells. *Dev Neurosci* 1993;**15**:289—98.
42. Strange K, Emma F, Paredes A, et al. Osmoregulatory changes in myo-inositol content and Na+/myo-inositol cotransport in rat cortical astrocytes. *Glia* 1994;**12**:35—43.
43. Kruse B, Hanefeld F, Christen HJ, et al. Alterations of brain metabolites in metachromatic leukodystrophy as detected by localized proton magnetic resonance spectroscopy *in vivo*. *J Neurol* 1993;**241**:68—74.

44. Kaminogo M, Ishimaru H, Morikawa M, et al. Diagnostic potential of short echo time MR spectroscopy of gliomas with single-voxel and point-resolved spatially localised proton spectroscopy of brain. *Neuroradiology* 2001;**43**:353—63.
45. Alger JR, Frank JA, Bizzi A, et al. Metabolism of human gliomas: assessment with H-1 MR spectroscopy and F-18 fluorodeoxyglucose PET. *Radiology* 1990;**177**:633—41.
46. Bruhn H, Michaelis T, Merboldt KD, et al. On the interpretation of proton NMR spectra from brain tumours *in vivo* and *in vitro*. *NMR Biomed* 1992;**5**:253—8.
47. Fulham MJ, Bizzi A, Dietz MJ, et al. Mapping of brain tumor metabolites with proton MR spectroscopic imaging: clinical relevance. *Radiology* 1992;**185**:675—86.
48. Meyerand ME, Pipas JM, Mamourian A, et al. Classification of biopsy-confirmed brain tumors using single-voxel MR spectroscopy. *AJNR Am J Neuroradiol* 1999;**20**:117—23.
49. Fountas KN, Kapsalaki EZ, Gotsis SD, et al. *In vivo* proton magnetic resonance spectroscopy of brain tumors. *Stereotact Funct Neurosurg* 2000;**74**:83—94.
50. Tamiya T, Kinoshita K, Ono Y, et al. Proton magnetic resonance spectroscopy reflects cellular proliferative activity in astrocytomas. *Neuroradiology* 2000;**42**:333—8.
51. Wilken B, Dechent P, Herms J, et al. Quantitative proton magnetic resonance spectroscopy of focal brain lesions. *Pediatr Neurol* 2000;**23**:22—31.
52. Gupta RK, Cloughesy TF, Sinha U, et al. Relationships between choline magnetic resonance spectroscopy, apparent diffusion coefficient and quantitative histopathology in human glioma. *J Neurooncol* 2000;**50**:215—26.
53. Lehnhardt FG, Rohn G, Ernestus RI, et al. 1H- and (31)P-MR spectroscopy of primary and recurrent human brain tumors *in vitro*: malignancy-characteristic profiles of water soluble and lipophilic spectral components. *NMR Biomed* 2001;**14**: 307—17.
54. Tedeschi G, Lundbom N, Raman R, et al. Increased choline signal coinciding with malignant degeneration of cerebral gliomas: a serial proton magnetic resonance spectroscopy imaging study. *J Neurosurg* 1997;**87**:516—24.
55. Shimizu H, Kumabe T, Tominaga T, et al. Noninvasive evaluation of malignancy of brain tumors with proton MR spectroscopy. *AJNR Am J Neuroradiol* 1996;**17**:737—47.
56. Daumas-Duport C, Scheithauer B, O'Fallon J, et al. Grading of astrocytomas. A simple and reproducible method. *Cancer* 1988;**62**:2152—65.
57. Law M, Yang S, Wang H, et al. Glioma grading: sensitivity, specificity, and predictive values of perfusion MR imaging and proton MR spectroscopic imaging compared with conventional MR imaging. *AJNR Am J Neuroradiol* 2003;**24**: 1989—98.
58. Tzika AA, Astrakas LG, Zarifi MK, et al. Spectroscopic and perfusion magnetic resonance imaging predictors of progression in pediatric brain tumors. *Cancer* 2004;**15**(100): 1246—56.
59. Castillo M, Smith JK, Kwock L. Correlation of myo-inositol levels and grading of cerebral astrocytomas. *AJNR Am J Neuroradiol* 2000;**21**:1645—9.
60. Yang D, Korogi Y, Sugahara T, et al. Cerebral gliomas: prospective comparison of multivoxel 2D chemical-shift imaging proton MR spectroscopy, echoplanar perfusion and diffusion-weighted MRI. *Neuroradiology* 2002;**44**:656—66.
61. Poptani H, Kaartinen J, Gupta RK, et al. Diagnostic assessment of brain tumours and non-neoplastic brain disorders *in vivo* using proton nuclear magnetic resonance spectroscopy and artificial neural networks. *J Cancer Res Clin Oncol* 1999;**125**:343—9.
62. Moller-Hartmann W, Krings T, Brunn A, et al. Proton magnetic resonance spectroscopy of neurocytoma outside the ventricular region—case report and review of the literature. *Neuroradiology* 2002;**44**:230—4.
63. Shimizu H, Kumabe T, Shirane R, et al. Correlation between choline level measured by proton MR spectroscopy and Ki-67 labeling index in gliomas. *AJNR Am J Neuroradiol* 2000;**21**:659—65.
64. Dowling C, Bollen AW, Noworolski SM, et al. Preoperative proton MR spectroscopic imaging of brain tumors: correlation with histopathologic analysis of resection specimens. *AJNR Am J Neuroradiol* 2001;**22**:604—12.
65. McKnight TR, von dem Bussche MH, Vigneron DB, et al. Histopathological validation of a three-dimensional magnetic resonance spectroscopy index as a predictor of tumor presence. *J Neurosurg* 2002;**97**:794—802.
66. Nelson SJ, McKnight TR, Henry RG. Characterization of untreated gliomas by magnetic resonance spectroscopic imaging. *Neuroimaging Clin N Am* 2002;**12**:599—613.
67. Kwock L, Smith JK, Castillo M, et al. Clinical applications of proton MR spectroscopy in oncology. *Technol Cancer Res Treat* 2002;**1**:17—28.
68. Lin A, Bluml S, Mamelak AN. Efficacy of proton magnetic resonance spectroscopy in clinical decision making for patients with suspected malignant brain tumors. *J Neurooncol* 1999; **45**:69—81.
69. Li X, Lu Y, Pirzkall A, et al. Analysis of the spatial characteristics of metabolic abnormalities in newly diagnosed glioma patients. *J Magn Reson Imaging* 2002;**16**:229—37.
70. Howe FA, Barton SJ, Cudlip SA, et al. Metabolic profiles of human brain tumors using quantitative *in vivo* 1H magnetic resonance spectroscopy. *Magn Reson Med* 2003;**49**:223—32.
71. Howe FA, Opstad KS. 1H MR spectroscopy of brain tumours and masses. *NMR Biomed* 2003;**16**:123—31.
72. Bronen RA. Epilepsy: the role of MR imaging. *AJR Am J Roentgenol* 1992;**159**:1165—74.
73. Bourgeois BFD. General concepts of medical intractibility. In: Luders HO, editor. *Epilepsy surgery*. New York: Raven Press; 1992. p. 77—81.
74. Bruton C. *The neuropathology of temporal lobe epilepsy*. Oxford: Oxford University Press; 1988.
75. Berkovic SF, Andermann F, Olivier A, et al. Hippocampal sclerosis in temporal lobe epilepsy demonstrated by magnetic resonance imaging. *Ann Neurol* 1991;**29**:175—82.
76. Gates JR, Cruz-Rodriguez R. Mesial temporal sclerosis: pathogenesis, diagnosis, and management. *Epilepsia* 1990; **31**(Suppl. 3):S55—66.
77. Jackson GD, Berkovic SF, Tress BM, et al. Hippocampal sclerosis can be reliably detected by magnetic resonance imaging. *Neurology* 1990;**40**:1869—75.
78. Miller BL, Moats RA, Shonk T, et al. Alzheimer disease: depiction of increased cerebral myo-inositol with proton MR spectroscopy. *Radiology* 1993;**187**:433—7.
79. Soher BJ, Doraiswamy PM, Charles HC. A review of 1H MR spectroscopy findings in Alzheimer's disease. *Neuroimaging Clin N Am* 2005;**15**:847—52. xi.
80. den Heijer T, Sijens PE, Prins ND, et al. MR spectroscopy of brain white matter in the prediction of dementia. *Neurology* 2006;**66**:540—4.
81. Metastasio A, Rinaldi P, Tarducci R, et al. Conversion of MCI to dementia: role of proton magnetic resonance spectroscopy. *Neurobiol Aging* 2006;**27**:926—32.
82. Kantarci K, Smith GE, Ivnik RJ, et al. 1H magnetic resonance spectroscopy, cognitive function, and apolipoprotein E genotype in normal aging, mild cognitive impairment and Alzheimer's disease. *J Int Neuropsychol Soc* 2002;**8**:934—42.
83. Doraiswamy PM, Charles HC, Krishnan KR. Prediction of cognitive decline in early Alzheimer's disease. *Lancet* 1998; **352**:1678.

84. Kubo H, Harada M, Sakama M, et al. Reproducibility of metabolite concentration evaluated by intraclass correlation coefficient using clinical MR apparatus. *J Comput Assist Tomogr* 2003;**27**:449—53.
85. Barker PB, Hearshen DO, Boska MD. Single-voxel proton MRS of the human brain at 1.5T and 3.0T. *Magn Reson Med* 2001; **45**:765—9.
86. Al-Okaili RN, Krejza J, Wang S, et al. Advanced MR imaging techniques in the diagnosis of intraaxial brain tumors in adults. *RadioGraphics* 2006;**26**(Suppl.1): S173—89.
87. Al-Okaili RN, Krejza J, Woo JH, et al. Intraaxial brain masses: MR imaging-based diagnostic strategy—initial experience. *Radiology* 2007;**243**:539—50.